LONG VALLEY OBSERVATORY QUARTERLY REPORTS
COMBINED January-June 2008

Long Valley Observatory
U.S. Geological Survey
Volcano Hazards Program, MS 910
345 Middlefield Rd., Menlo Park, CA 94025

http://lvo.wr.usgs.gov

This report is a preliminary description of unrest in Long Valley caldera and Mono-Inyo Craters region of eastern California. Information contained in this report should be regarded as preliminary and is not be cited for publication without approval by the Scientist in Charge of the Long Valley Observatory. The views and conclusions contained in this document do not necessarily represent the official policies, either express or implied, of the U.S. Government.

LONG VALLEY OBSERVATORY QUARTERLY REPORTS
January-June 2008

CONTENTS

SUMMARY FOR JANUARY-JUNE 2008

The relative quiescence in Long Valley caldera that began in the spring of 1998 continued through the first half of 2008. The resurgent dome, which essentially stopped inflating in early 1998 and showed minor subsidence (of about 1 cm) through 2001, was followed by gradual inflation through 2002. The deformation pattern since 2003 has been characterized by gradual subsidence that appears to have flattened out in early 2007. The center of the resurgent dome remains some 75 cm higher than prior to the onset of unrest in 1980. Seismic activity within the caldera was low with no earthquakes as large as magnitude M=2.0. Activity beneath Mammoth Mountain was somewhat higher with four M>2 earthquakes, three of which occurred in a small swarm on June 29. Seismic activity throughout the greater Long Valley region included 11 earthquakes with magnitudes greater than M = 3.0, the largest of which was a M – 3.9 event on June 29 located 2 miles east of Convict Lake. This earthquake produced perceptible shaking in Mammoth Lakes and vicinity. The carbon dioxide flux in the vicinity of Mammoth Mountain remains elevated but has shown evidence of a fluctuating decline since 1995. Recent measurement document isolated areas of elevated CO_2 flux within the caldera along the southwestern margin of the resurgent dome in Basalt Canyon and the Shady Rest fumarole. Sporadic episodes of geysering in Hot Creek that began in May 2006 has continued to decline with the most active areas now located down-stream from the parking lot overlook.

Up-to-date plots for most of the data summarized here are available on the Long Valley Observatory web pages (http://lvo.wr.usgs.gov).

EARTHQUAKES *(D.P. Hill and A.M. Pitt)*

Note: S*eismic activity in this report uses the automatic computer-generated (Earthworm) solutions rather than the final hand- check (CUSP processing) solutions. The computer-generated epicentral locations and magnitude estimates have become increasingly reliable with time, and they do not suffer from backlogs that can develop in CUSP processing due to an abrupt increase in the rate of earthquake activity elsewhere in northern California.*

LONG VALLEY CALDERA AND MAMMOTH MOUNTAIN ACTIVITY:
Low levels of earthquake activity beneath Long Valley caldera and Mammoth Mountain continued through the first six months of 2008. Minor activity beneath Mammoth Mountain included a M=2.3 earthquake at 2:51 AM on April 7 and a swarm on June 29 that included magnitude three M = 2 events between 8:33 and 8:44 PM. None of the earthquakes within the caldera during this period had magnitudes as large as M=2.0.

SIERRA NEVADA ACTIVITY
As has been true since 1999, earthquake activity in the Sierra Nevada block south of the caldera continues at a higher rate than within the caldera with most of the activity concentrated in a band extending from the southern margin of the caldera for some 20 km to the south-southwest (Figures S1-S7). A sequence of earthquakes clustered between Big McGee Lake and Grinnell Lake (~14 km south of the caldera) between April 7 – 25 included two M = 2.5 earthquakes on the 7th and 22nd (Figure S4). The most energetic activity included a M=3.2 earthquake beneath Round Valley at 10:04 PM on March 9 and a sequence of three M>3 earthquakes in June along the seismicity band extending south of the caldera (Figure S6). The latter developed as a northward progression beginning with a M=3.1 at 7:57 AM on June 2 located just north of the April 7-25 sequence near Big McGee Lake. This was followed by a M=3.2 earthquake at 10:26 PM on June 26 located 2 miles east of Mount Baldwin. The largest earthquake in this progression (and the first six months of the year) was a M=3.9 event at 7:44 AM on June 29 located 2 miles east of Convict Lake. This earthquake produced perceptible shaking throughout the Mammoth Lakes area.

REGIONAL ACTIVITY
A M=3.2 earthquake occurred beneath Round Valley at 10:04 PM on March 9. An earthquake sequence on April 27 beneath the southwestern margin of the Volcanic Tableland (4 miles east of the Round Valley earthquake and one mile south of the Pleasant Valley reservoir in the Owens Gorge) included M=3.4 and 3.5 earthquakes at 6:23 and 6:25 PM, respectively. This was followed by a M=3.0 earthquake in the same area at 1:47 AM on May 2 (Figures S3, S5, S6).

Elsewhere, low level activity continues in the Adobe Hills area (10 to 15 miles east of Mono Lake) with some twelve M>2.5 earthquakes including M=3.0 and M=3.3 earthquakes on January 15 and April 23, respectively.

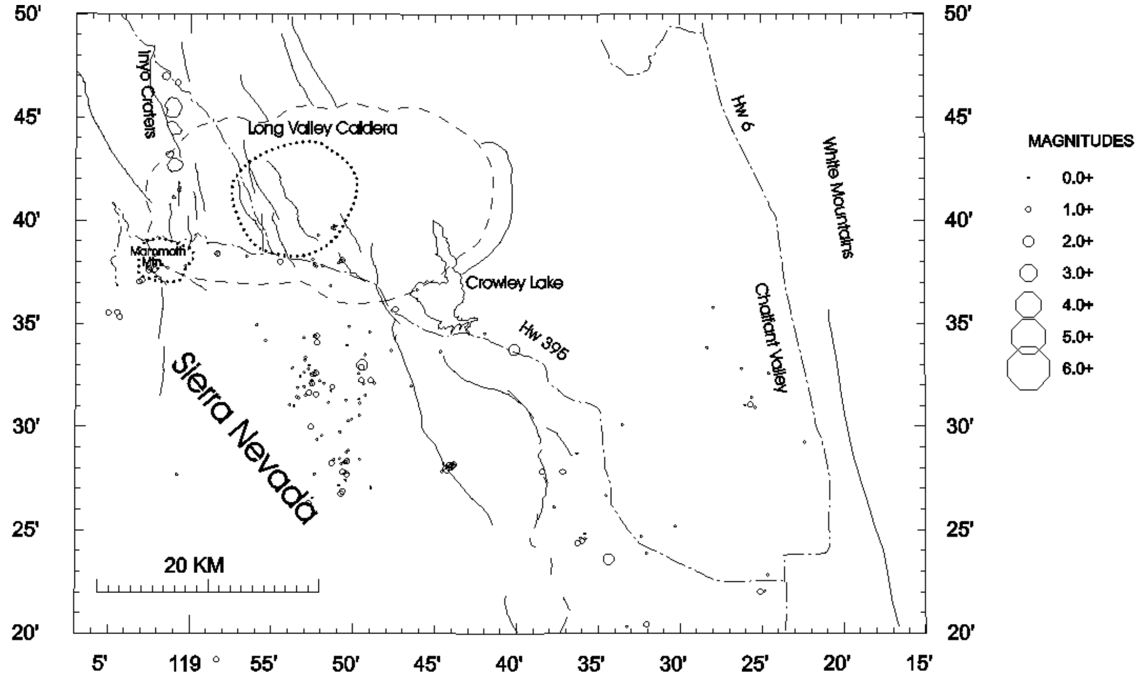

Figure S1: Earthquake epicenters (ALL) in the Long Valley region for Jan. 2008

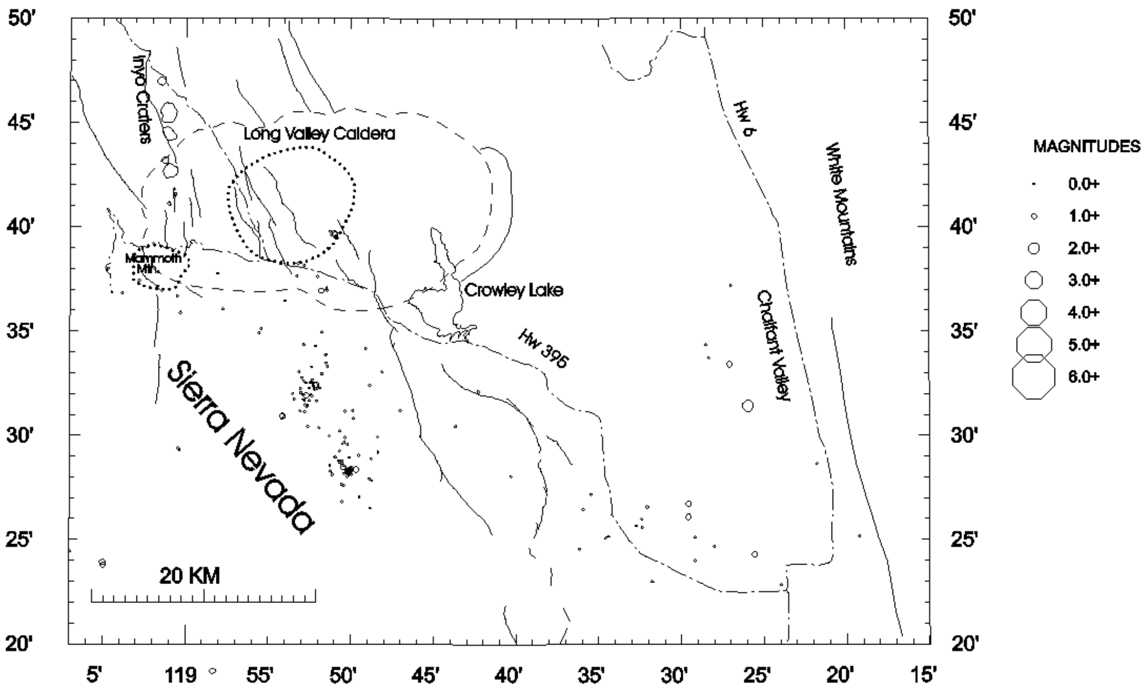

Figure S2: Earthquake epicenters (ALL) in the Long Valley region for Feb. 2008

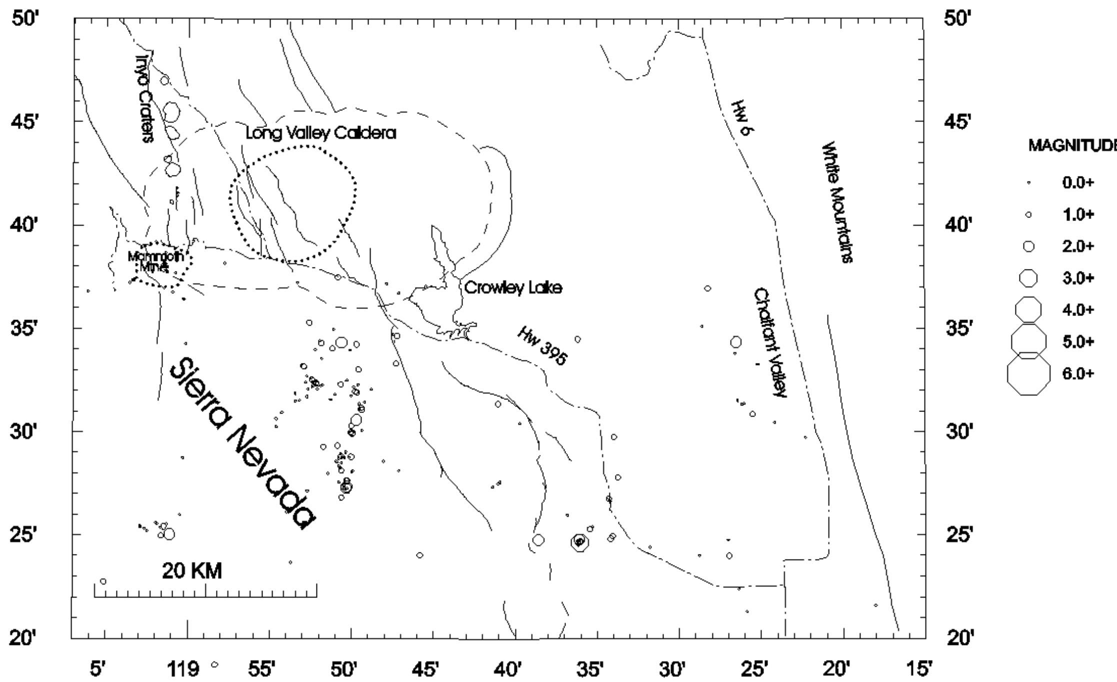

Figure S3: Earthquake epicenters (ALL) in the Long Valley region for Mar. 2008

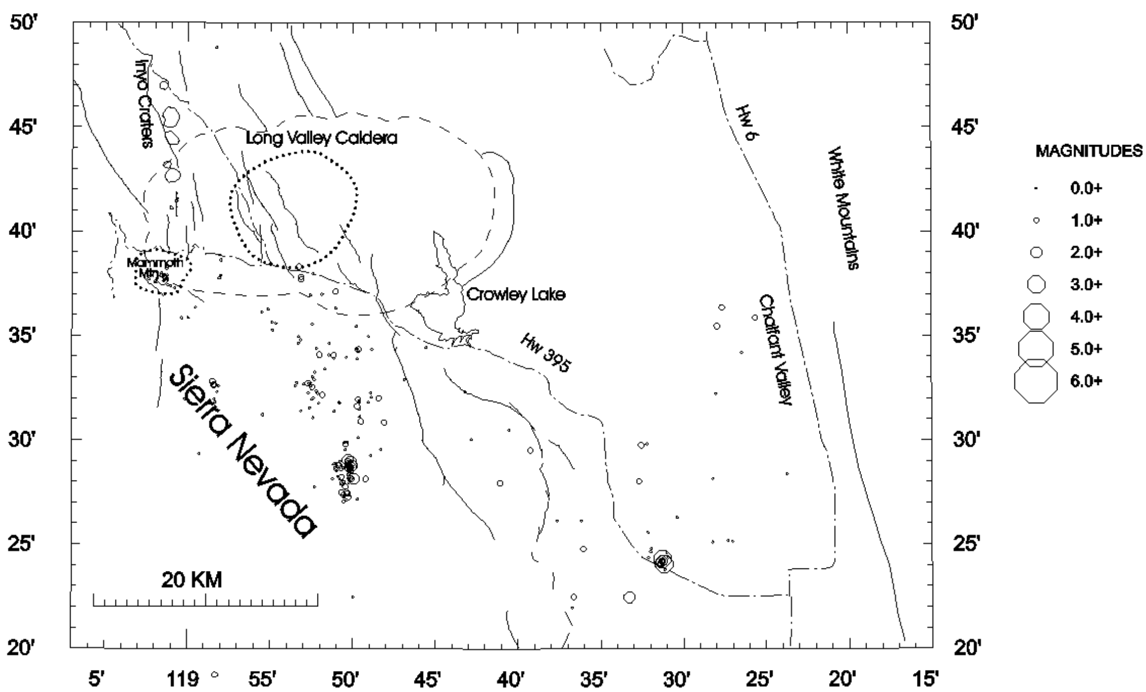

Figure S4: Earthquake epicenters (ALL) in the Long Valley region for Apr. 2008

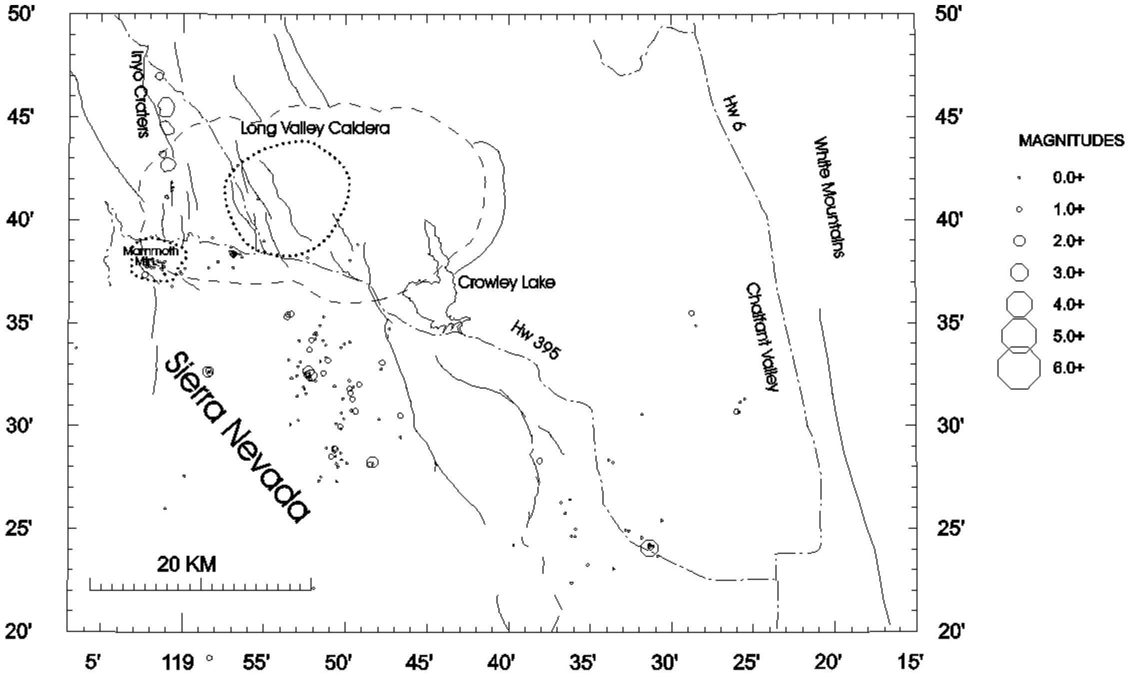

Figure S5: Earthquake epicenters (ALL) in the Long Valley region for May 2008

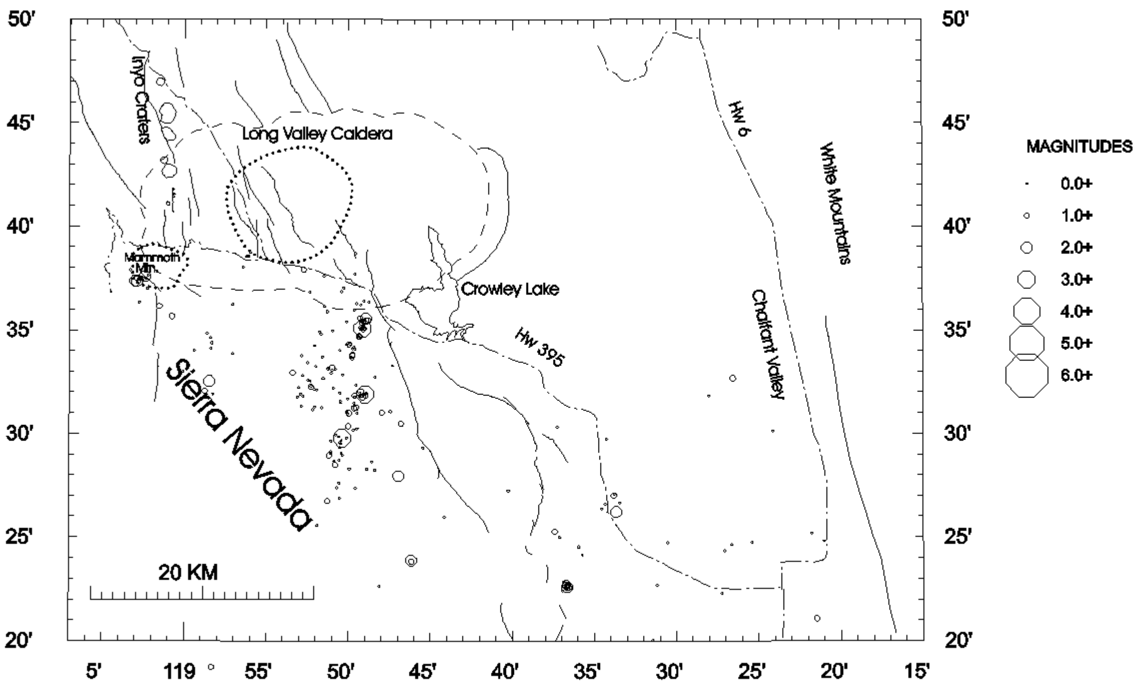

Figure S6: Earthquake epicenters (ALL) in the Long Valley region for Jun. 2008

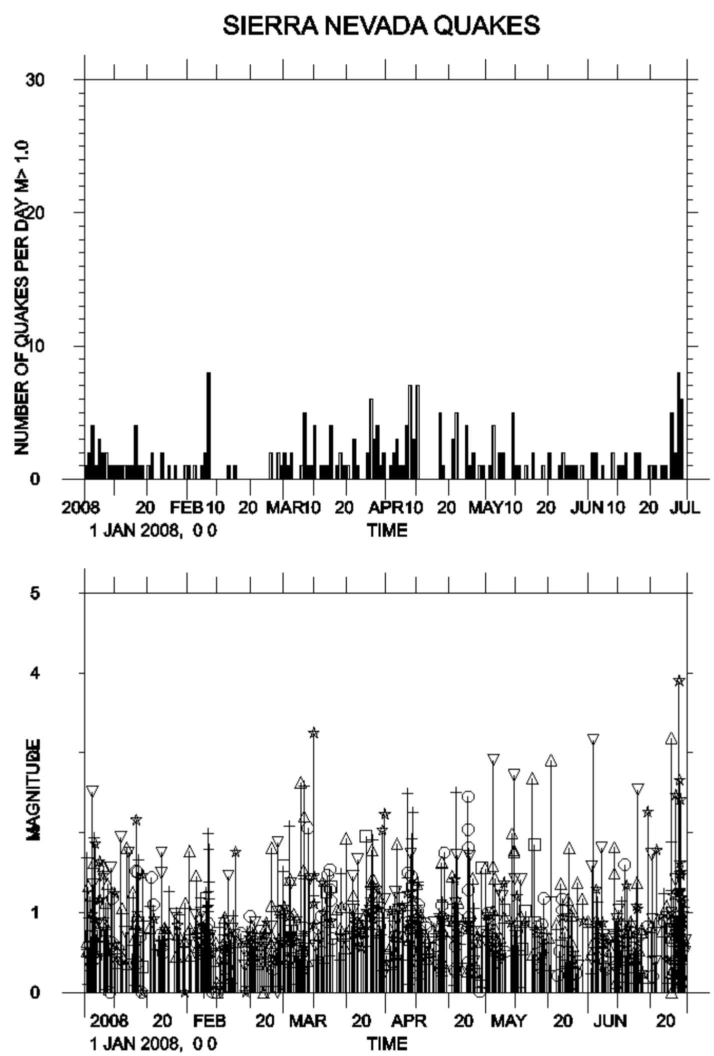

Figure S7: Temporal occurrence of earthquakes (ALL) in geographic subregions of area shown on figures S1 through S6. Top: number of >M1 events per day. Bottom: event magnitudes proportional to line length with focal depth indicated by symbol at top of line.

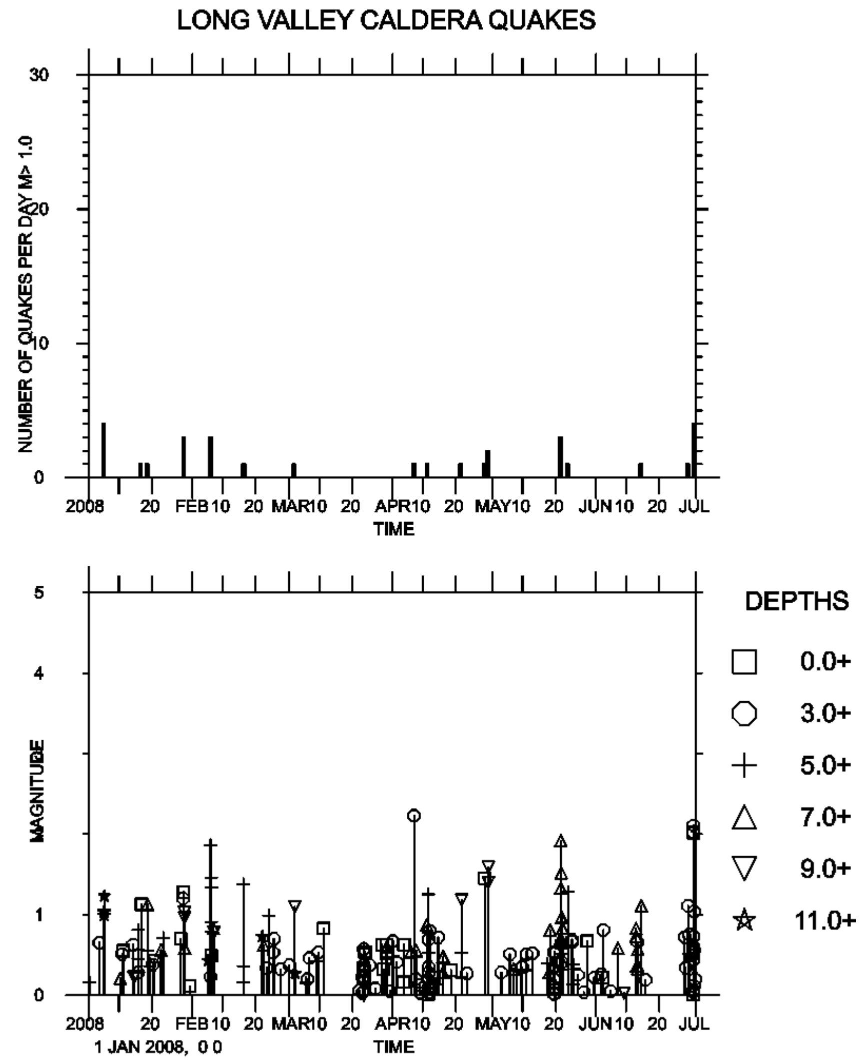

Figure S8 : Temporal occurrence of earthquakes (ALL) in geographic subregions of area shown on figures S1 through S6. Top: number of >M1 events per day. Bottom: event magnitudes proportional to line length with focal depth indicated by symbol at top of line.

DEFORMATION

SUMMARY OF EDM AND GPS MEASUREMENTS

John Langbein, Stuart Wilkinson, Mike Lisowski, Eugene Iwatsubo, and Jerry Svarc

Over the past 7 years, 18 GPS (Global Position System) receivers have been installed within and near the Long Valley Caldera. The locations of the 12 receivers within the caldera are shown in Figure G1. The close correlation of variations in baseline lengths between the EDM measurements that began in 1984 and the GPS measurements, the first of which began in 1999 (Figures G1, G2, G3), has allowed us to discontinue the expensive, labor-intensive EDM measurement in October of 2006. In the future, we will rely entirely on the GPS measurements.

Results from the GPS data indicate that, following the rapid 10-cm inflation associated with the 1997-98 episode of caldera unrest, the resurgent dome has remained relatively stable with only minor fluctuations in the baseline lengths through mid-2008. The most notable of these fluctuations involved a gradual, 3-cm extension (uplift) episode through most of 2002 (Figure G2). Over the long term, the center of the resurgent dome has remained some 75 cm higher than prior to the onset of caldera unrest in 1980 (Figure G3). Also see; http://lvo.wr.usgs.gov/monitoring/index.html#deformation

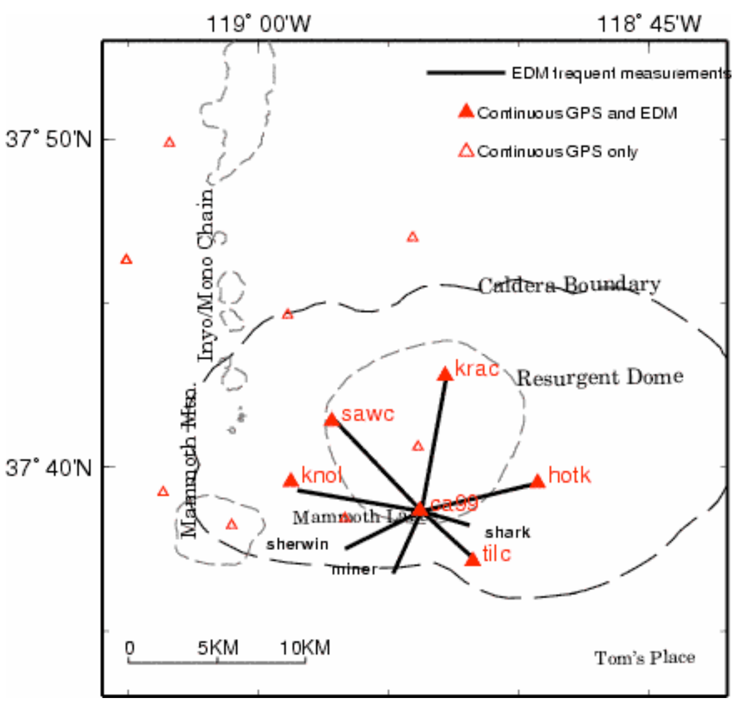

Figure G-1 Map showing 2-color EDM baselines

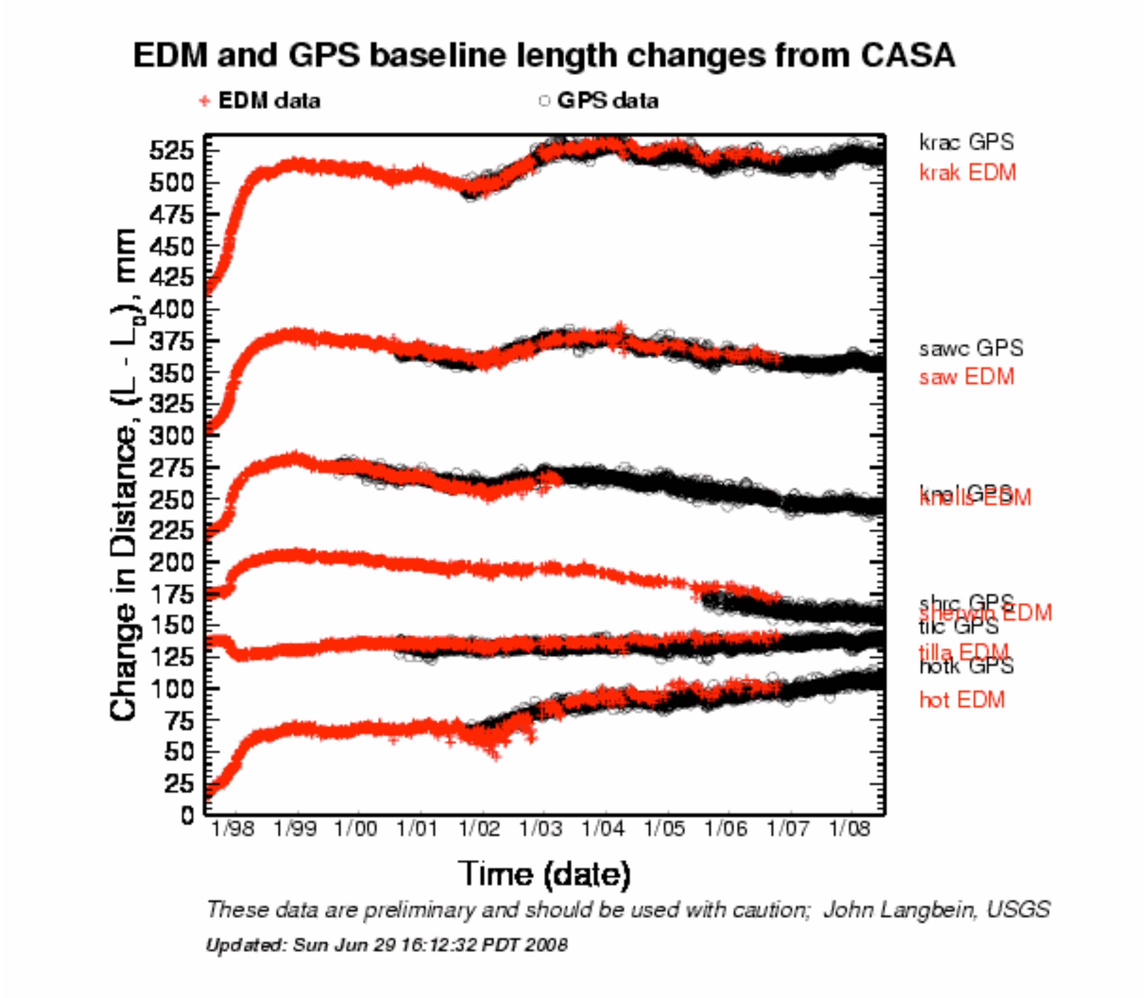

Figure G2.Line-length changes for the EDM baselines (red crosses) measured from CASA for the period February 12, 1997 through June 29, 2008 compared with continuous GPS data for the same lines (black circles). Note that the EDM measurements were discontinued in October 2006.

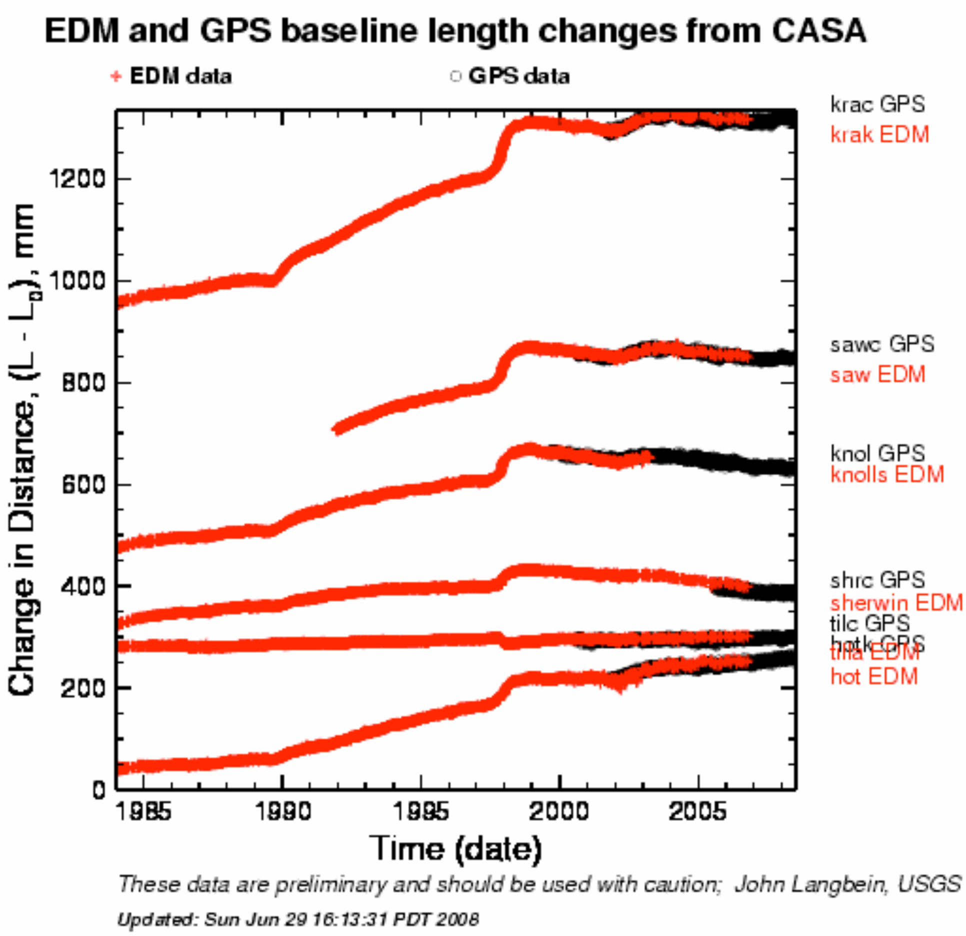

Figure G3. Line-length changes for the EDM baselines (red crosses) measured from CASA for the period June 1984 through June 29, 2008 compared with continuous GPS data for the same lines (black circles). Note that the EDM measurements were discontinued in October 2006.

CONTINUOUS BOREHOLE STRAIN MEASUREMENTS (Malcolm Johnston, Doug Myren, and Stan Silverman)

Instrumentation

Dilational strain measurements are being recorded continuously at the Devil's Postpile (POP), Motorcross (MX) near the western moat boundary in the south moat, Big Springs (BS) just outside the norhtern caldera boundary, and at Phillips (PLV1), just to the north of the town of Mammoth Lakes. The site locations are shown in Figure D1. The instruments are Sacks-Evertson dilational strain meters and consist of stainless steel cylinders filled with silicon oil that are cemented in the ground at a depth of about 200m. Changes in volumetric strain in the ground are translated into displacement and voltage by a expansion bellows attached to a linear voltage displacement transducer.

This instrument is described in detail by Sacks et al.(*Papers Meteol. Geophys*. ,22, 195, 1971).

Data from the strainmeters are transmitted using satellite telemetry every 10 minutes to a host computer in Menlo Park. The data are also transmitted with 24-bit seismic telemetry together with 3-component seismic data to Menlo Park.

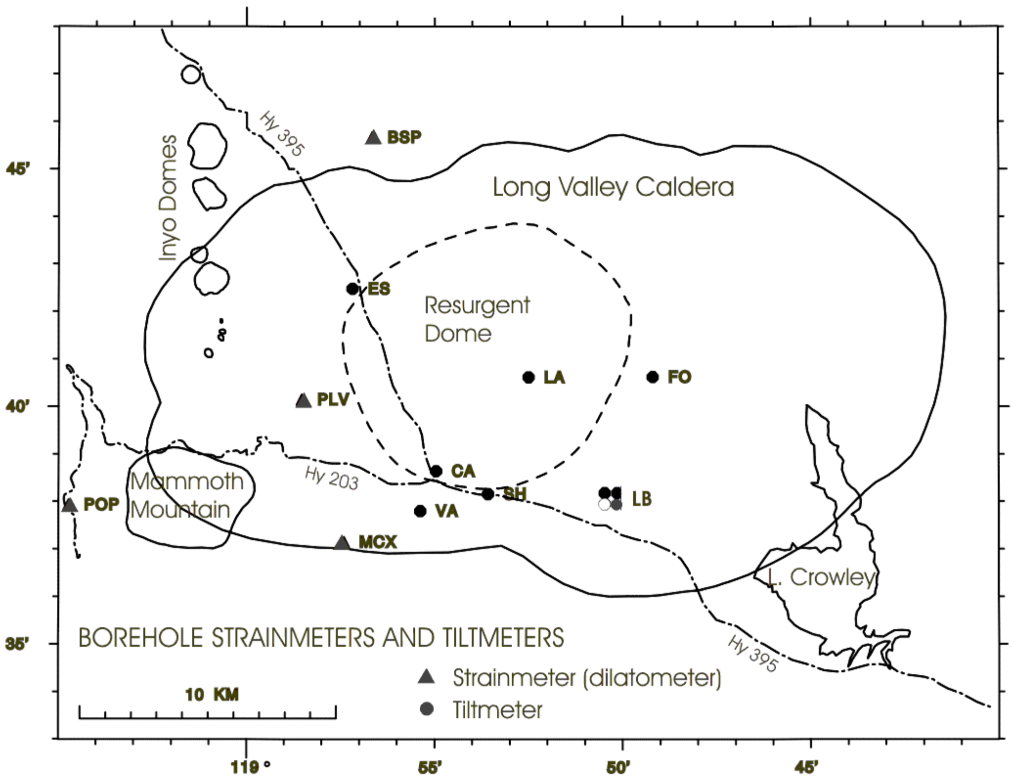

.
Figure D1. Locations of dilatometers and tiltmeters.

Highlights

The data during this quarter has been relatively quiet at all sites other than small changes at MX in March and PLV in early May. Pressure corrected data are shown in Figure D2. Pore pressure at Postpile was not available this period due to failure in the sensor. This was repaired in August 2008.

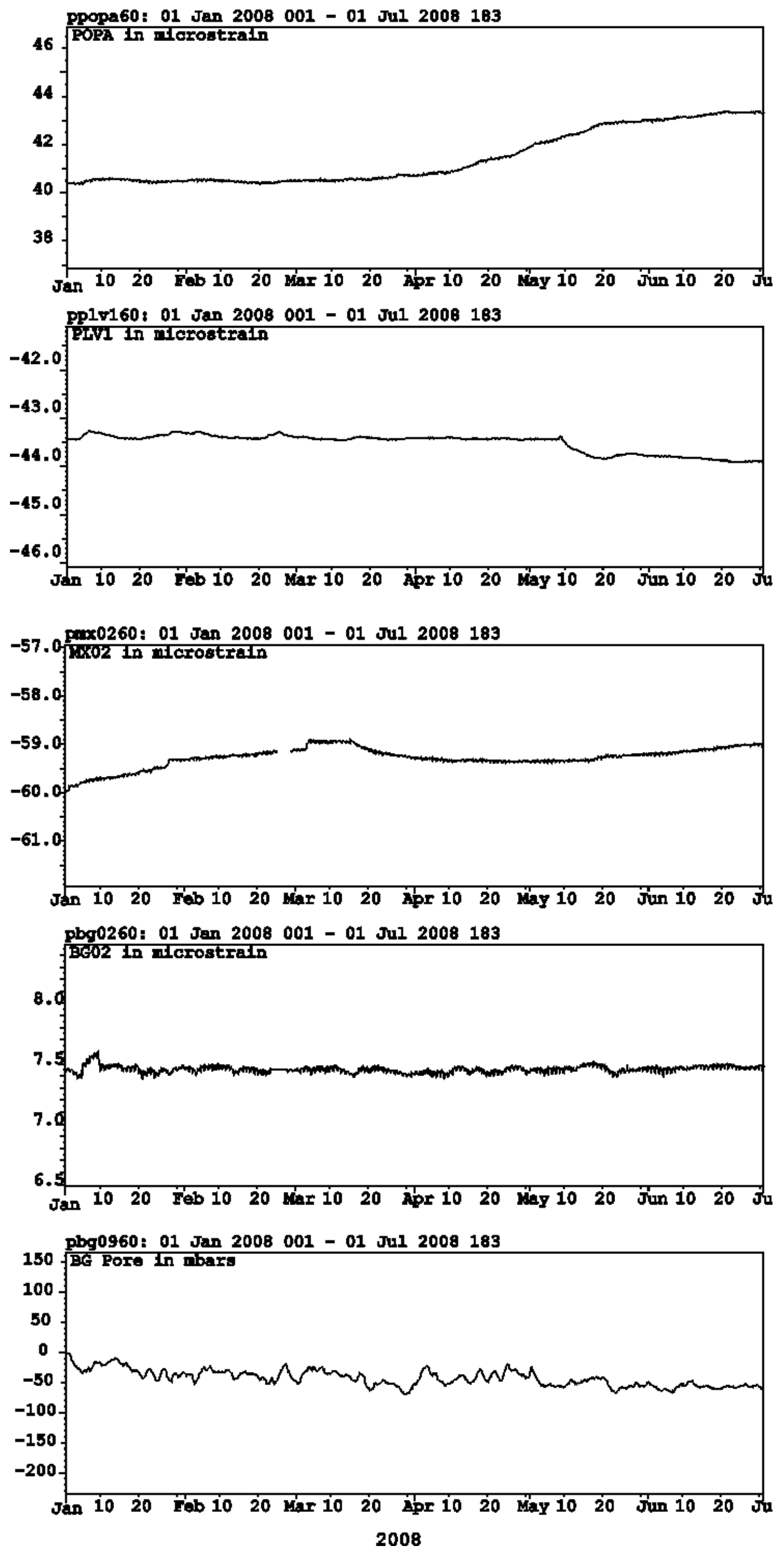

Figure D2. Dilatational strain for borehole dilatometers POPA, PLV1, MX, and BS f or January – June, 2008.

TILT MEASUREMENTS (Mal Johnston, Roger Bilham, Doug Myren and Stuart Wilkensen)

Instrumentation

Instruments recording crustal tilt in the Long Valley caldera are of two types - 1) a long-base (LB) instrument in which fluid level is measured in fluid reservoirs separated by about 500 m and connected by pipes, which was constructed by Roger Bilham of the University of Colorado, and 2) borehole tiltmeters that measure the position of a bubble trapped under a concave lens. For tiltmeter locations, see Figure D1. Real time plots of the data from these instruments can be viewed at http://quake.wr.usgs.gov/QUAKE/longv.html.

All data are transmitted by satellite to the USGS headquarters in Menlo Park, CA Data samples are taken every 10 minutes. Plots of the changes in tilt as recorded on each of these tiltmeters are shown in Figures T1-T3. Removal of re-zeros, offsets, problems with telemetry and identification of instrument failures is difficult, tedious and time-consuming task. In order to have a relatively up-to-date file of data computer algorithms have been written that accomplish most of these tasks most of the time. Detailed discussion or detailed analysis usually requires hand checking of the data. Flat sections in the data usually denote a failure in the telemetry. Gaps denote missing data. All instruments are scaled using tidally generated scale factors.

Highlights

Fig T1 shows the long base data from June 1, 2007 to Jan 1, 2008. No changes of note are apparent. Data from the tiltmeters in the deep boreholes at Big Springs and Motorcross are shown in Figure T2, and data from the short base tiltmeters are shown in Figures T3. Very little of geophysical interest occurred this period.

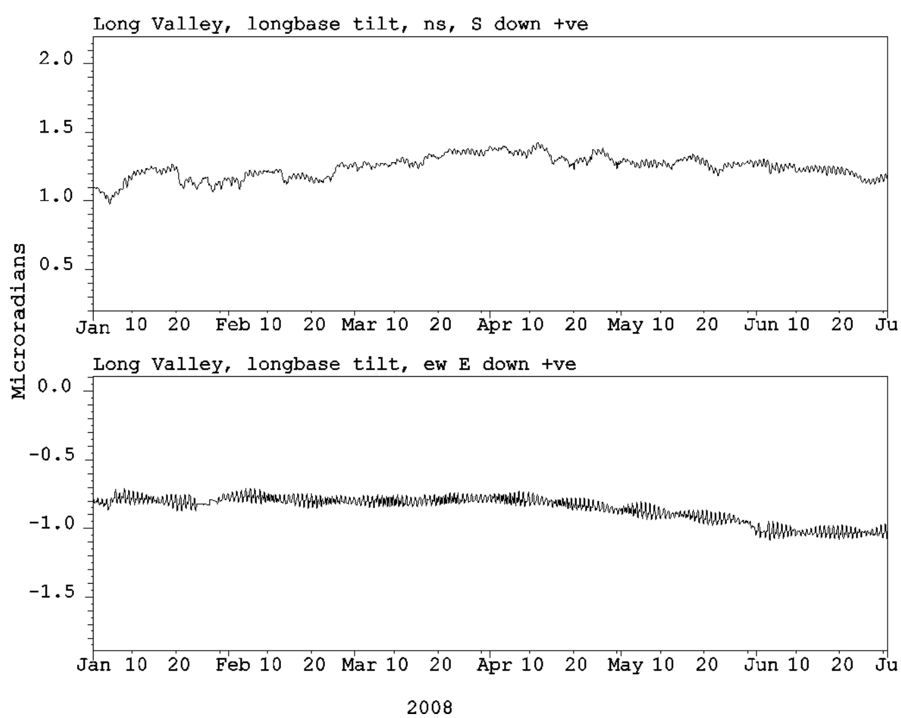

Figure T1. East-west and north-south components of the long-base tiltmeter for January – June, 2008. Positive slopes indicate tilt down the south and east, respectively.

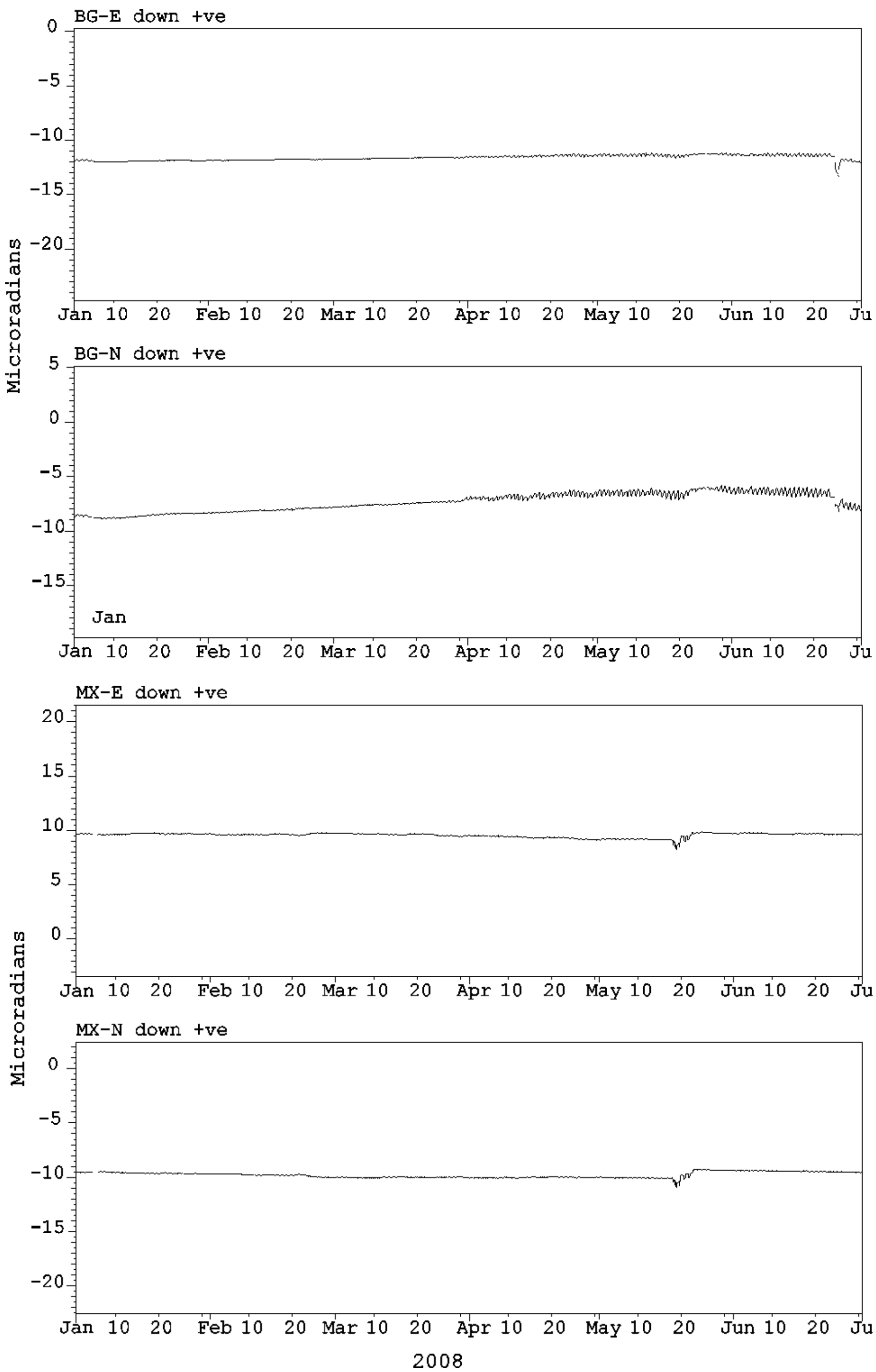

Figure T2. East-west and north-south components for the borehole tiltmeters installed with the Big Springs (BS) and Motocross (MX) dilatometers for January – June, 2008.

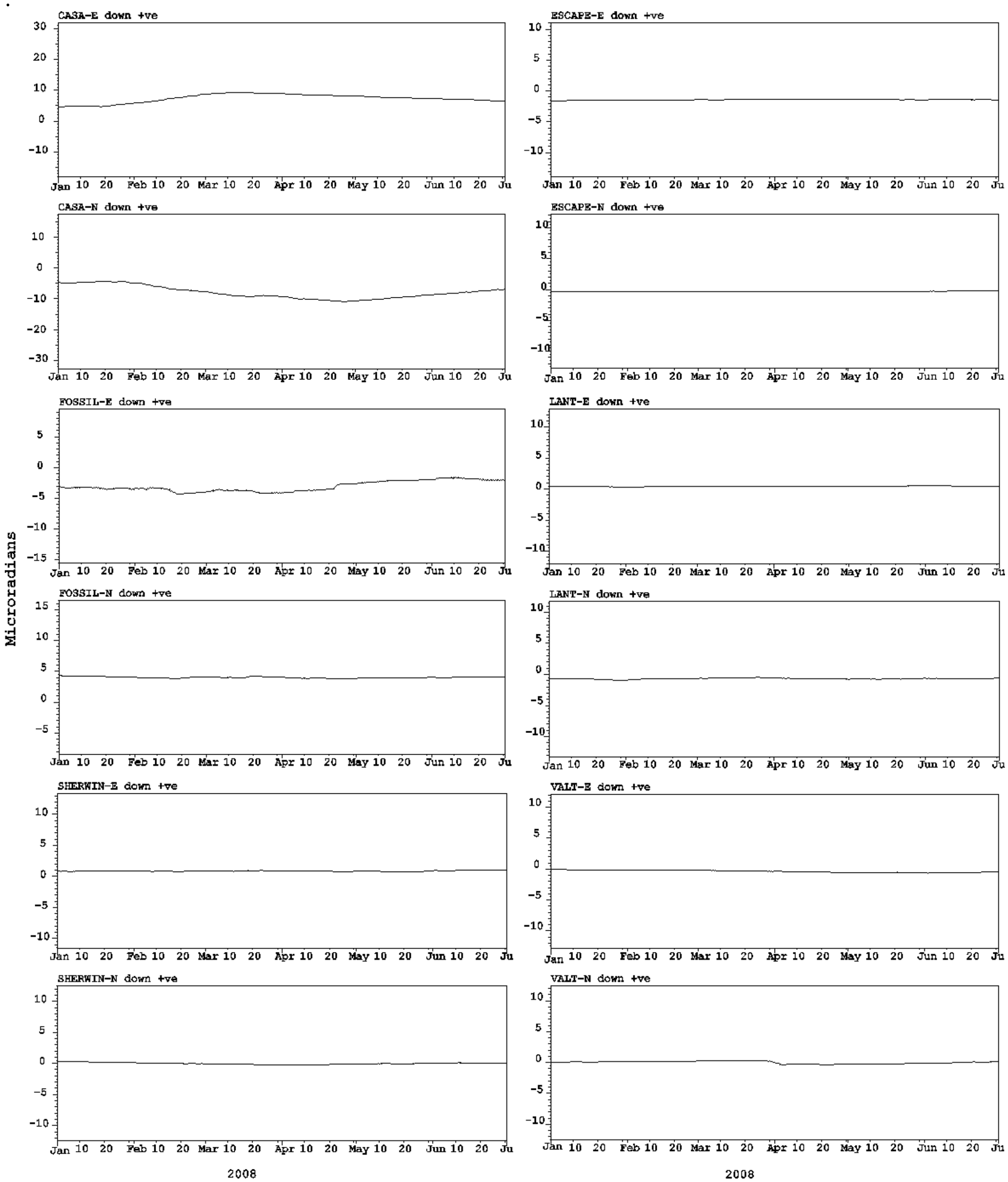

Figure T4. East-west and north-south tilt components for the shallow borehole tiltmeters for January – June, 2008. See Figure D1 for locations.

MAGNETIC MEASUREMENTS (M.J.S. Johnston, S. Wilkinson, Doug Myren, Y. Sassai, and Y. Tanaka)

Background
Local magnetic fields at 18 sites in the Long Valley Caldera are transmitted via satellite telemetry to Menlo Park every 10 minutes. These and other data provide continuous 'real-time' monitoring in this region through the low-frequency data system. The location of these sites is shown on Figure M1. Temporal changes in local magnetic field are isolated using simple differencing techniques.

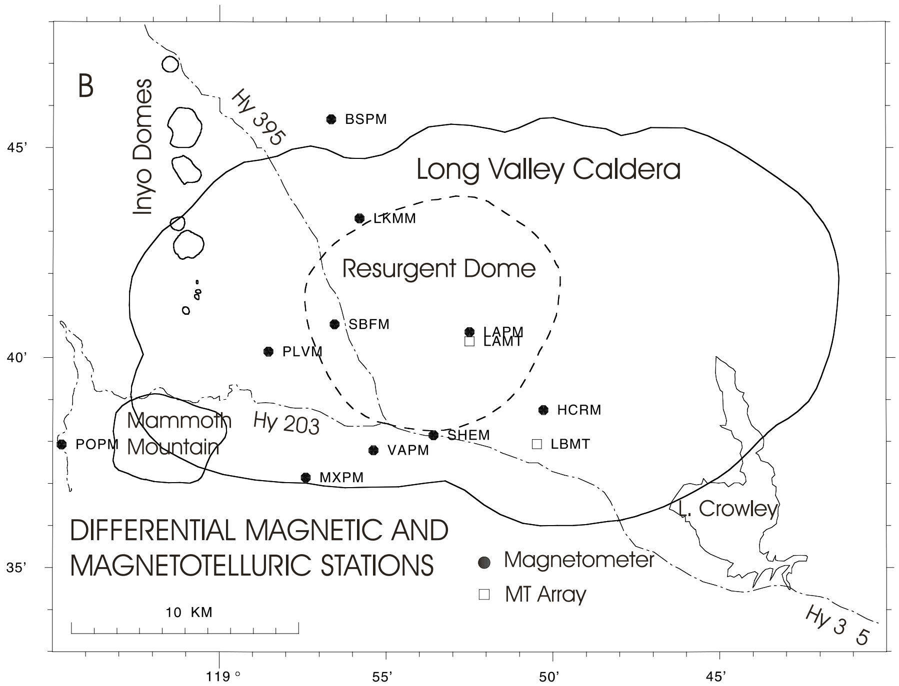

Figure M1. Locations of differential magnetic field stations within Long Valley caldera. The reference station MGS (not shown) is located along Highway 395 approximately 20 km southeast of the caldera.

Data:
Plots of daily averaged data from the telemetered magnetometer stations in and near the caldera are shown in Figures M2.. As these instrument are getting old we are having great difficulty keeping them alive. Dedicated work by Stuart Wilkinson is greatly appreciated.

Highlights:
Nothing unusual during this quarter.

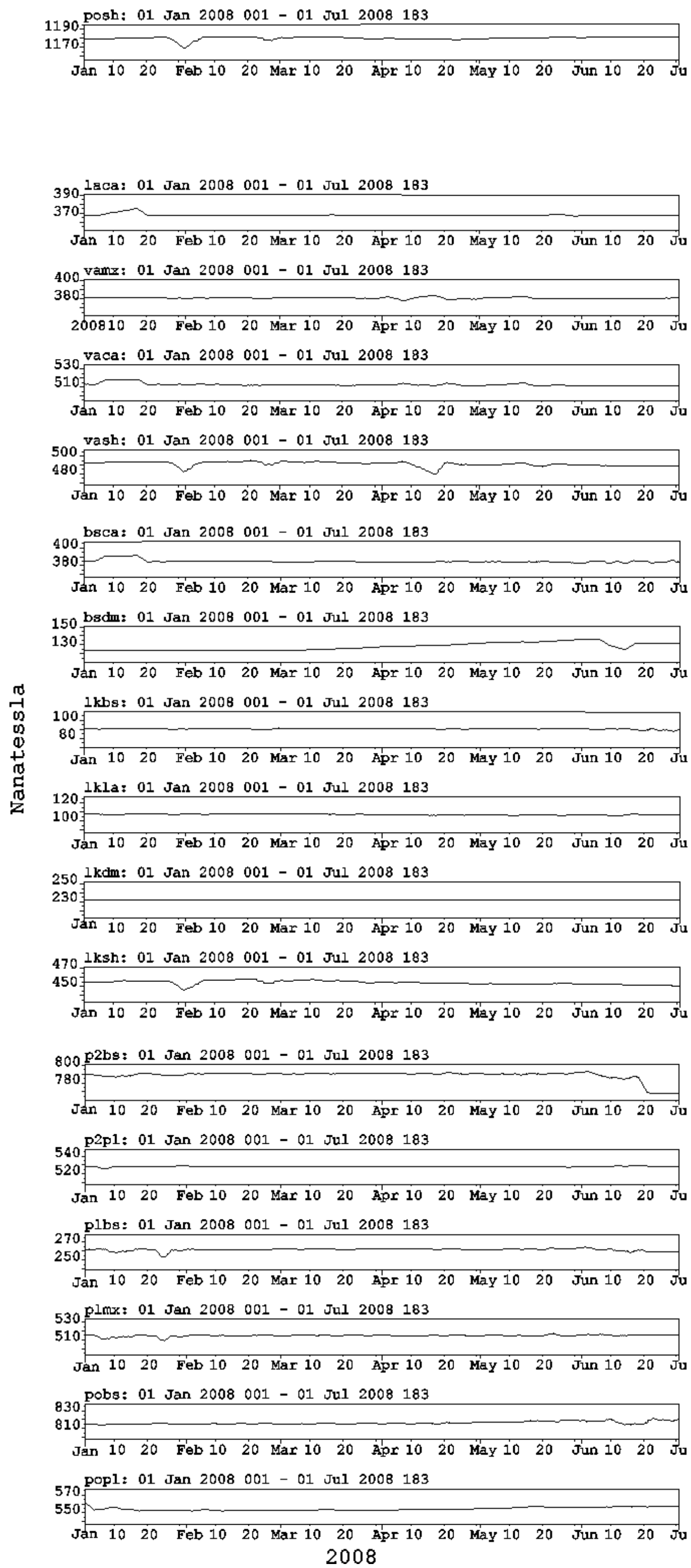

Figure M2. Differential magnetometer data for the stations shown in Figure M1 for January – June, 2008.

INTRACALDERA DIFFUSE CO_2 STUDIES (Deborah Bergfeld and William Evans).

Background
Early studies of diffuse CO_2 emissions from 13 areas of localized vegetation kill within Long Valley caldera (LVC) showed some of the most active areas are situated in and around fault zones in Basalt Canyon on the southern margin of the resurgent dome (Fig. 1). Unlike tree kill areas on Mammoth Mountain which are related to cold CO_2 emissions, all of the kill areas within LVC are associated with thermal ground. CO_2 emissions at these sites show the influence of both shallow and deep processes. Recent perturbations in the upflow of CO_2 are related to changes in the shallow hydrothermal system, while carbon isotope data show the CO_2 has the same deep source as that discharging from the fumarole on Mammoth Mountain.

In June 2006 we combined two areas from the previous study at Basalt Canyon (BC) to create a long-term diffuse CO_2 monitoring site. At present the BC site covers approximately 18,000 m^2, although the grid may need to be enlarged as a new area of tree kill continues to increase in size. In September 2006 we established a second monitoring site about 2 km northwest of BC near the Shady Rest fumarole (SRF). The fumarole is a weak gas vent that is the westernmost surface expression of the Long Valley hydrothermal system. The SRF monitoring grid is located about 0.5 km north of two new geothermal production wells and contains several patches of slightly thermal ground near the fumarole and in the north and east portions of the grid.

Methods
CO_2 flux measurements are made using an accumulation chamber and a field-portable infrared CO_2 analyzer. Soil temperature data are collected at each site and are typically measured at a depth of 10 cm. At each grid the average flux ($g\ m^{-2}\ d^{-1}$) is calculated based on 1000 sequential Gaussian simulations (sGs) of the measured flux data (see Lewicki et al, GRL (34), 2007). For each survey the total CO_2 emissions in metric tonnes per day ($t\ d^{-1}$) are calculated by multiplying the average CO_2 flux by the grid area.

Heat and gas upflow
Plots of soil temperature *vs.* CO_2 flux for both grids show considerable scatter with a general positive correlation between the upflow of gas and heat (Fig. 2). Due to the presence of high flux sites that lack a thermal signature the average correlation coefficients at SRF and BC are generally low, 0.4 and 0.1 (for all surveys) respectively. At the BC grid the high-flux / low-temperature sites are located along the slopes of the northwest canyon wall suggesting that at these sites the lack of correlation is due to steam condensing at depth.

Table 1 shows the statistical parameters for flux surveys at the BC grid from 2004 to 2008 and at the SRF grid from 2006 to 2008. Discussion herein is based on results from sGs calculations, and results from the arithmetic average are shown in Table 1 for completeness. Although there is some variation over time, the average flux is generally higher at BC as compared to the SRF grid. Over the course of study the average flux at BC grid is around 300 $g\ m^{-2}\ d^{-1}$ as compared to about 150 $g\ m^{-2}\ d^{-1}$ for SRF. The coefficients of variation (standard deviation divided by the average) show a similar degree of variation in the flux at both grids and is typical of that found in our early study. There are no observed trends in the flux data from either grid (Fig. 3). Using the average area for each grid and the average flux the areally adjusted emissions from BC and SRF are 5 and 10 $t\ d^{-1}$.

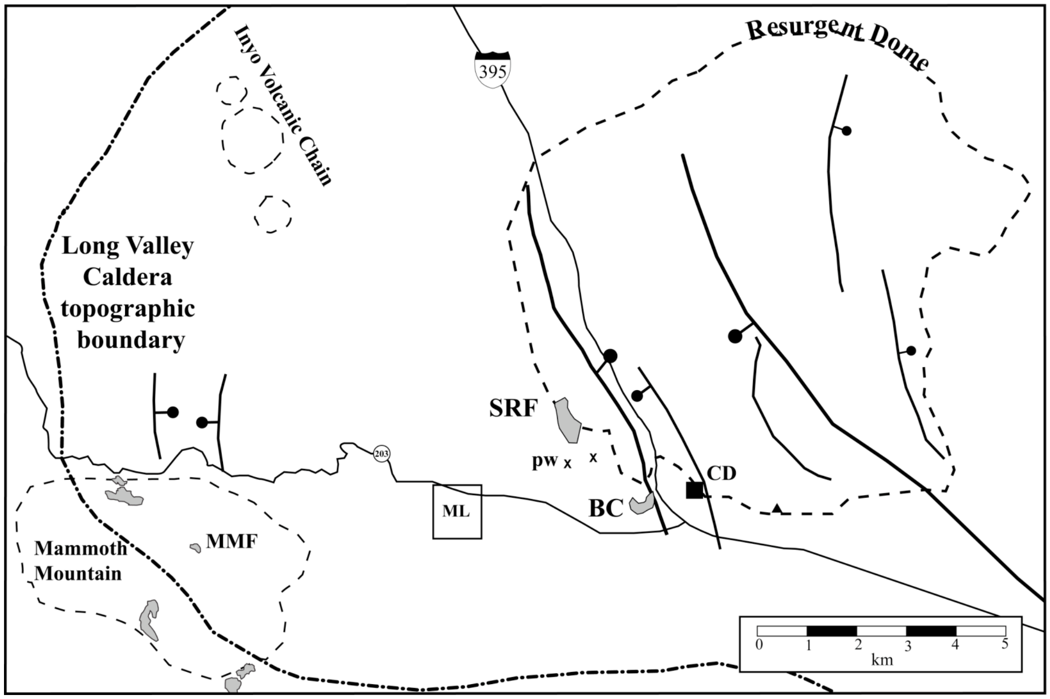

Figure 1. Sketch map showing the location for the BC (Basalt Canyon) and SRF (Shady Rest Fumarole grids relative to tree kill areas on Mammoth Mountain. ML = Mammoth Lakes, MMF = Mammoth Mountain Fumarole, CD = Casa Diablo geothermal plant, pw indicates locations of new geothermal drill holes.

Figure 2. Relations between soil temperatures and CO_2 flux at the BC and SRF grids in September 2006.

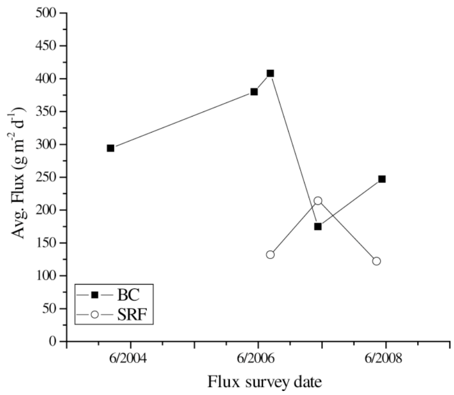

Figure 3. Variation in the average emissions at the BC grid (5 surveys) and the SRF grid (3 surveys).

Table 1. Statistical data from field surveys of CO_2 flux at the BC and SRF grids.

Table 1A					sGs Estimate		Arithmetic Estimate	
Grid	Date	N	Area	Avg. Flux	Avg. Emissions	Emissions range	Avg. Flux	Avg. Emissions
			m^2	$g\ m^{-2}\ d^{-1}$	$t\ d^{-1}$	$t\ d^{-1}$	$g\ m^{-2}\ d^{-1}$	$t\ d^{-1}$
BC	March 2004	58	15700	294	4.6	2 - 7	314	4.9
BC	June 2006	66	15100	380	5.7	2 - 11	318	4.8
BC	Sept. 2006	64	14775	408	6.0	1 - 13	286	4.2
BC	June 2007	83	22425	175	3.9	1 - 8	208	4.7
BC	June 2008	83	18050	247	4.5	1 - 9	239	4.3
Minimum			14775	175	3.9		208	4
Maximum			22425	408	6.0		318	5
Coeff. Variation				0.32				
Areal Adj. Avg.					**5**			

Table 1B					sGs Estimate		Arithmetic Estimate	
Grid	Date	N	Area	Avg. Flux	Avg. Emissions	Emissions range	Avg. Flux	Avg. Emissions
			m^2	$g\ m^{-2}\ d^{-1}$	$t\ d^{-1}$	$t\ d^{-1}$	$g\ m^{-2}\ d^{-1}$	$t\ d^{-1}$
SRF	Sept. 2006	81	54875	132	7.2	4 - 10	132	7.2
SRF	June 2007	90	66525	214	14.2	9 - 19	212	14.1
SRF	May 2008	108	75925	122	9.2	6 - 12	116	8.8
Minimum			54875	122	7.2		116	7
Maximum			75925	214	14.2		212	14
Coeff. Variation				0.32				
Areal Adj. Avg.					**10**			

HYDROLOGIC MONITORING (*Chris Farrar, Jim Howle, and Michelle Sneed: U.S. Geological Survey, Carnelian Bay and Sacramento, CA).*

Hydrologic data collected for the USGS Volcanic Hazards Program in this report include ground-water level data from four wells; stream flow, water temperature, and specific conductance from one site on Hot Creek; and estimated thermal water discharge in Hot Creek Gorge (figure H1). Additional data are available on the web at -- http://lvo.wr.usgs.gov/HydroStudies.html or upon request – contact: *Chris Farrar at Carnelian Bay 530.546.0187.*

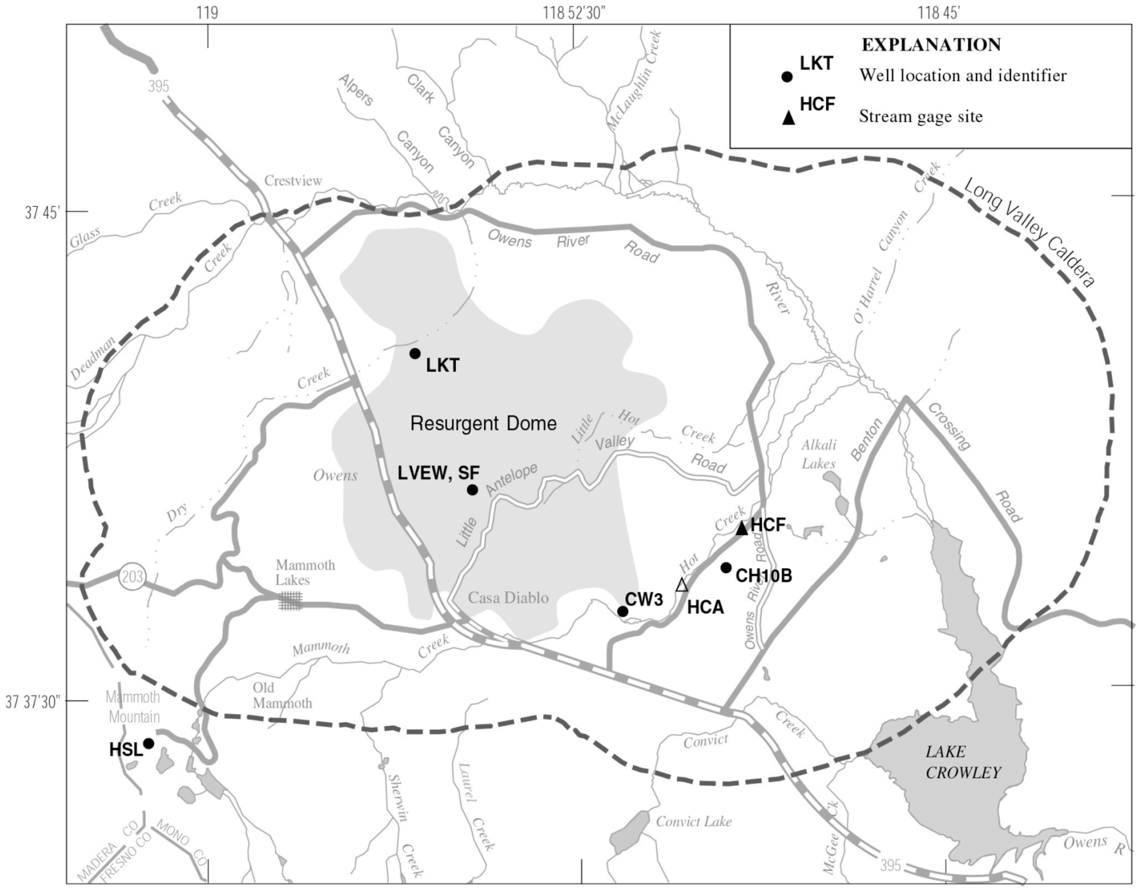

Figure H1—Hydrologic monitoring sites in Long Valley Caldera.

BACKGROUND

Ground-water levels in wells and the discharge of springs can change in response to strain in the Earth's crust. The network of wells and surface water sites provides hydrologic data that contributes to monitoring deformation and other changes caused from magmatic intrusions and earthquakes in Long Valley Caldera.

GROUND-WATER LEVEL MONITORING

Ground-water levels are measured continuously in four wells, LKT, LVEW, SF, and CH-10B (locations in figure H1), using pressure transducers that are either submerged below the water surface or placed above ground and sense back-pressure in a nitrogen-filled tube extending below the water surface. Barometric pressure is also measured at each site using pressure transducers. The data are recorded by on-site data loggers and telemetered on a three-hour transmit-cycle using the GOES satellite and receivers at Menlo Park and Sacramento. All sites are visited monthly to collect data from on-site recorders and to check instrument calibrations.

Data processing is done in the Sacramento Office. Records of barometric pressure are used in combination with the water-level records to determine aquifer properties from the observed water-level response to atmospheric loading and earth tides. The influences of barometric pressure changes and earth tides are removed from the water-level records. The result yields the filtered water-level record that may contain other hydraulic and crustal deformation signals. Filtered data for wells LKT and CH-10B are given in figures H2 and H3.

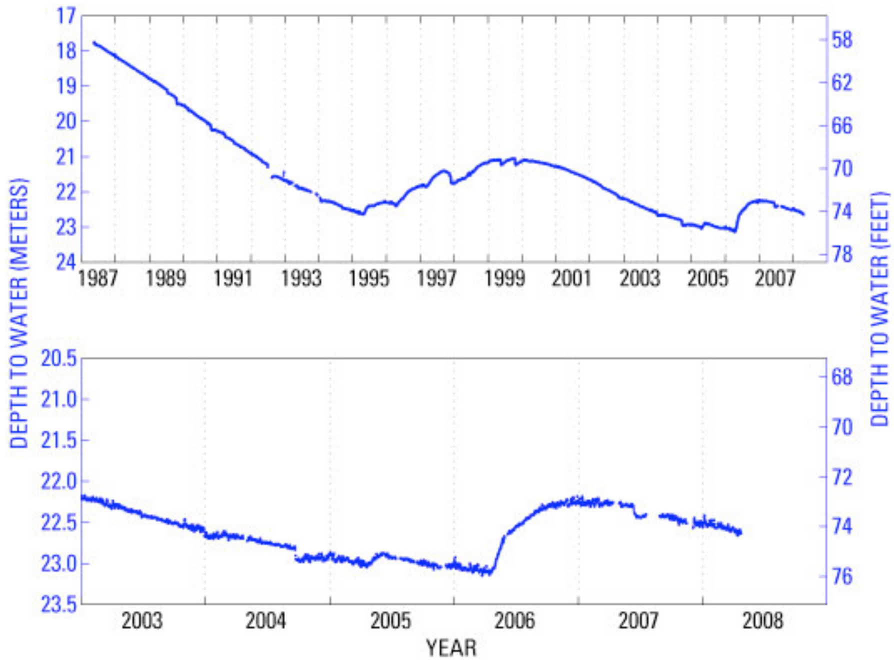

Figure H2. Hydrographs for well LKT, based on filtered daily mean values. The rise, beginning in mid-2006 is from a strong recharge pulse derived from the above average winter 2006 snow-pack. The decline in level that began in 2007 has continued into the first half of 2008 because of minimal recharge in this part of the caldera.

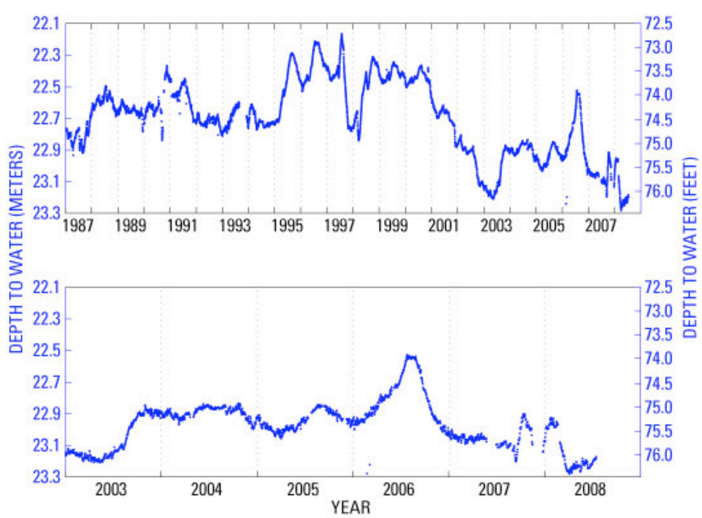

Figure H3. Hydrographs for well CH10B, based on filtered mean daily fluid levels. The large fluid level rise in mid-2006 is due to high recharge from above average precipitation during the winter of 2006. The fluid level oscillated about 0.2 m during the last half of 2007 and first part of 2008, then reached its lowest level in 21 years of observation. The oscillations in level are consistent with some of the shifting in locations of thermal spring discharge in Hot Creek Gorge.

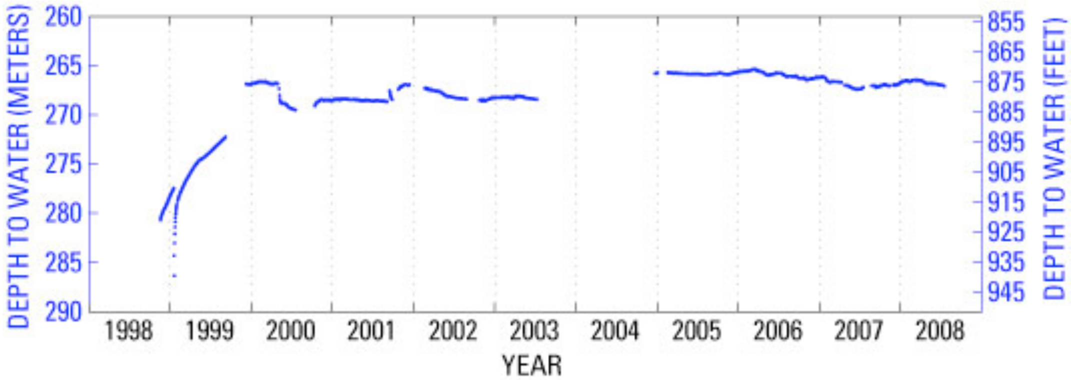

Figure H4. Unfiltered fluid levels in well LVEW.

The fluid level in well LVEW is controlled by the pressure in a fractured rock aquifer at a depth of about 3000 m below land surface and therefore is largely buffered against seasonal fluctuations.

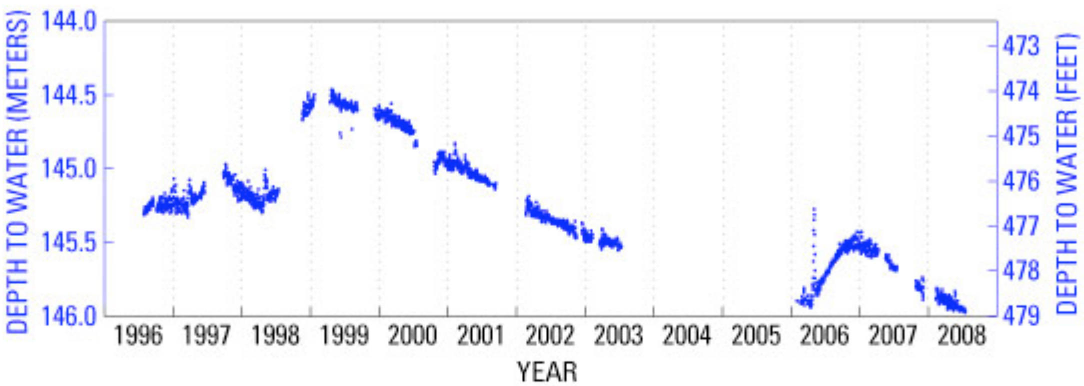

Figure H5. Unfiltered fluid levels in well SF, near LVEW.

The fluid level in well SF represents the hydraulic pressure in the upper 270 m of volcanic rock making up the resurgent dome. Fluid levels in SF respond to inter-annual patterns of precipitation and recharge. The fluid level dropped to its lowest level in 12 years of observation in June 2008.

SURFACE WATER MONITORING

Site HCF is located downstream from the thermal springs in Hot Creek Gorge (figure H1). Stage, water temperature, and specific conductance (figure H6) are recorded every 15-minutes. The data are recorded by an on-site data logger and telemetered every three hours. Specific conductance is a measure of total dissolved ionized constituents. Water at HCF is a mixture of thermal water from springs along Hot Creek and non-thermal water from the Mammoth Creek basin. Changes in specific conductance are related to changes in the mixing ratio of thermal and non-thermal components of stream flow. Water temperatures change in response to ambient temperatures and the mixing ratio.

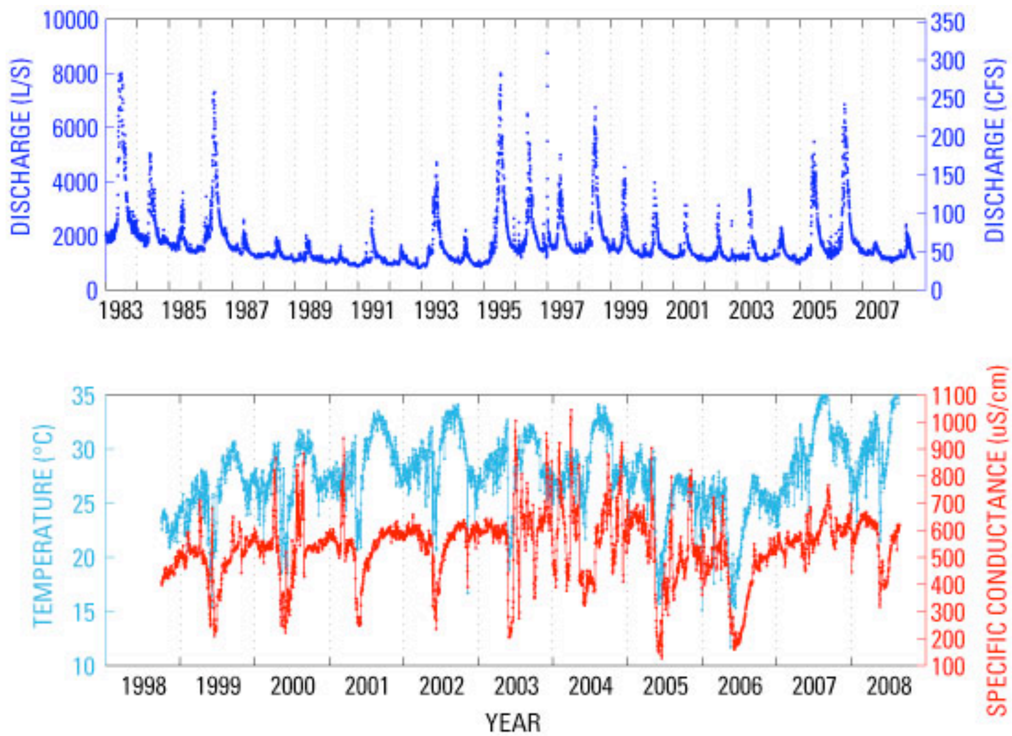

Figure H6. Discharge, water temperature, and specific conductance at Hot Creek Flume (HCF), based on daily mean data.

The effects of back to back winters with below average precipitation can be seen in the very small discharge peaks during spring runoff in 2007 and 2008. Water temperatures remain high because of the low flow conditions.

THERMAL WATER DISCHARGE ESTIMATE

Estimates of total thermal water discharge (figure H7) are computed from monthly measurements of discharge, and boron and chloride concentrations collected at a non-recording site (HCA) located upstream of the Hot Creek gorge thermal area and at site HCF downstream. The quantity of thermal water discharged to Hot Creek is known to vary in response to seasonal variations in precipitation, snow-melt, earthquakes, and other processes. It is believed that spring discharge may change in response to crustal strain.

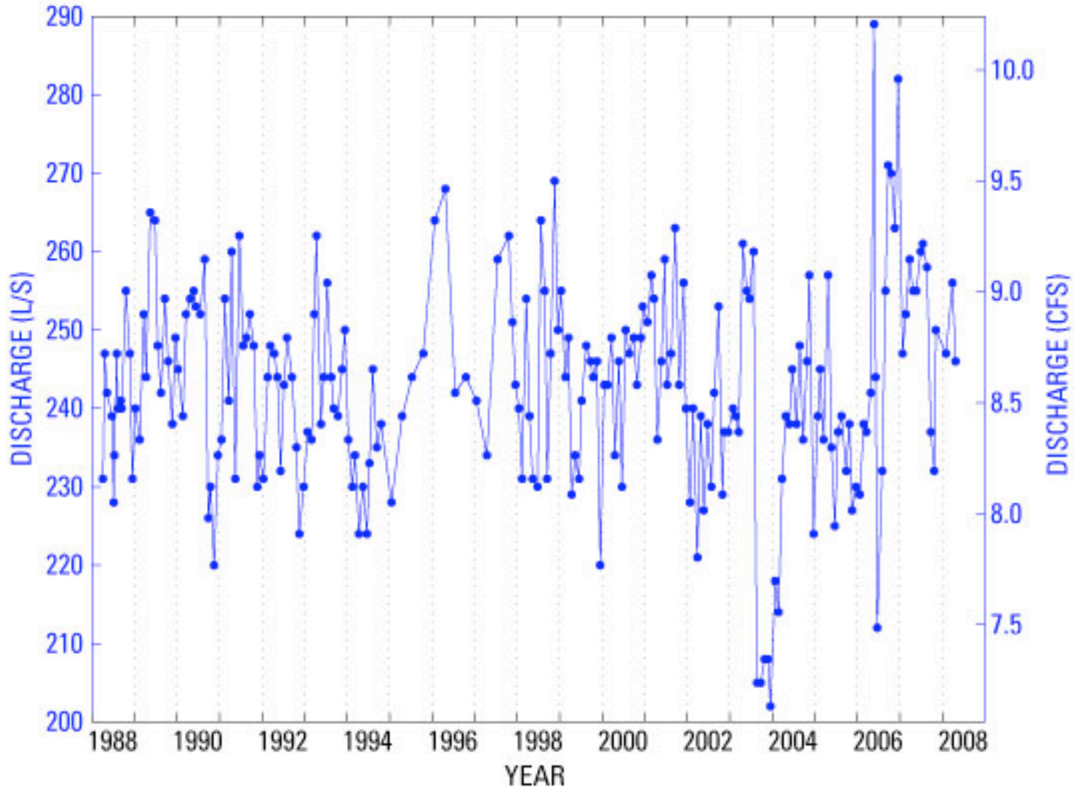

Figure H7. Estimated thermal water discharge for springs in Hot Creek Gorge.

Thermal springs in Hot Creek Gorge, throughout 2007 and into the first half of 2008, have continued to exhibit variability in discharge, temperatures, and vent locations. The vigorous fountaining-discharge from springs that began in May 2006 has been more subdued in 2007 and 2008. The median estimated total thermal water discharge of 252 L/s for 2006 to 2008 is slightly greater than the median of 244 L/s for 1985 to 2005. The shift in the locations of active spring vents along the banks of Hot Creek, from mostly along the left bank (northwest side) to mostly along the right bank is the most notable change in the springs. The U.S. Forest Service closure of the area for swimming remains in effect because of the unpredictable behavior of the springs and areas of soil instability along the banks of Hot Creek.